Supplementary file for: "Model-based super-resolution reconstruction for pseudo-continuous Arterial Spin Labeling"

Q. Beirinckx[a,d,*], P. Bladt[a,d], M. C. E. van der Plas[b], M. J. P. van Osch[b], B. Jeurissen[a,c,d], A. J. den Dekker[a,d] and J. Sijbers[a,d,*]

[a] *imec-Vision Lab, Department of Physics, University of Antwerp, Antwerp, Belgium*
[b] *C.J. Gorter MRI Center, Department of Radiology, Leiden University Medical Center, Leiden, The Netherlands*
[c] *Lab for Equilibrium Investigations and Aerospace, Department of Physics, University of Antwerp, Antwerp, Belgium*
[d] *μNEURO Research Centre of Excellence, University of Antwerp, Antwerp, Belgium*

ARTICLE INFO

Keywords:
arterial spin labeling
perfusion
CBF mapping
super-resolution
quantitative MRI
model-based reconstruction

ABSTRACT

This document includes supplementary material that complements the main body of the paper. In Section S1, we provide additional figures with results of the whole brain Monte Carlo simulation experiment, for the simulations without motion (Section S1.1) and with motion (Section S1.2).

*Corresponding author, Address: Vision Lab, University of Antwerp (CDE), Universiteitsplein 1, N.1.16, B-2610 Antwerpen, Belgium
quinten.beirinckx@uantwerpen.be (Q. Beirinckx)
ORCID(s): 0000-0002-5339-052X (Q. Beirinckx); 0000-0002-1294-9948 (P. Bladt); 0000-0003-2240-8405 (M. C. E. van der Plas); 0000-0001-7034-8959 (M. J. P. van Osch); 0000-0002-3488-9819 (B. Jeurissen); 0000-0002-0194-0198 (A. J. den Dekker); 0000-0003-4225-2487 (J. Sijbers)

S1. Whole brain simulation experiment

S1.1. Simulations without motion

As discussed in section 3.1.1 of the main body, noise settings for σ_0 and c in the simulated datasets were tuned to match the temporal SNR (tSNR) values observed in the conventional HR *in vivo* dataset (see Table 2 of the main body). Fig. S1 shows the voxel-wise tSNR map obtained from the conventional HR *in vivo* data alongside the tSNR maps of the datasets used in the simulation experiment, as well as a comparison in overall tSNR value. Note that for datasets 1 and 3, the tSNR increased approximately 4-fold as a result of the increased slice thickness of those images when using the SRR forward model (Eq. (1) of the main body), as signal scales linearly with the imaged volume. In addition, the process of simulating one noise realization of the single-PLD pCASL dataset for SRR (dataset 1) without unwanted motion is illustrated in Fig. S2.

Orthogonal slice views of the simulated 2D control images are visualized in Fig. S3, both for the pCASL data with high through-plane resolution (HR) and low through-plane resolution (LR), with or without the use of multiband (MB). For the LR data, two of the 24 slice orientation angles (0° and 90°) are shown, as defined in Fig. 1 of the main body. For comparison, and to appreciate resolution enhancements, the corresponding HR CBF map that was estimated from the simulated control-label images is also shown for each method. Furthermore, to ease a qualitative and visual comparison of the CBF map estimated by each method, Fig. S4 shows zoomed image regions to indicate noticeable CBF estimation differences compared to the ground truth CBF map (Ref). Finally, Fig. S5 and Fig. S6 show axial slices of the relative absolute bias and relative standard deviation maps, respectively, corresponding with the slice locations of Fig. 5 of the main body.

Dataset	Overall tSNR
Dataset 1	4.92
Dataset 2	1.21
Dataset 3	5.61
Dataset 4	1.64
Conventional HR (real) data	1.59

Figure S1: Coronal views and transverse slices of the voxel-wise temporal SNR maps of the simulated datasets 1-4, and as calculated from the conventional HR *in vivo* 2D EPI dataset (see Table 2 of the main body). Dashed lines are used to indicate transitions between multibands. Note that for the HR Datasets 2 and 4, and the Conventional HR Dataset, only a selection of 24 out of the 40 transverse slices is shown. For each dataset, the overall tSNR measure is indicated, which was calculated by taking the spatial mean inside a whole-brain mask of each voxel-wise tSNR map.

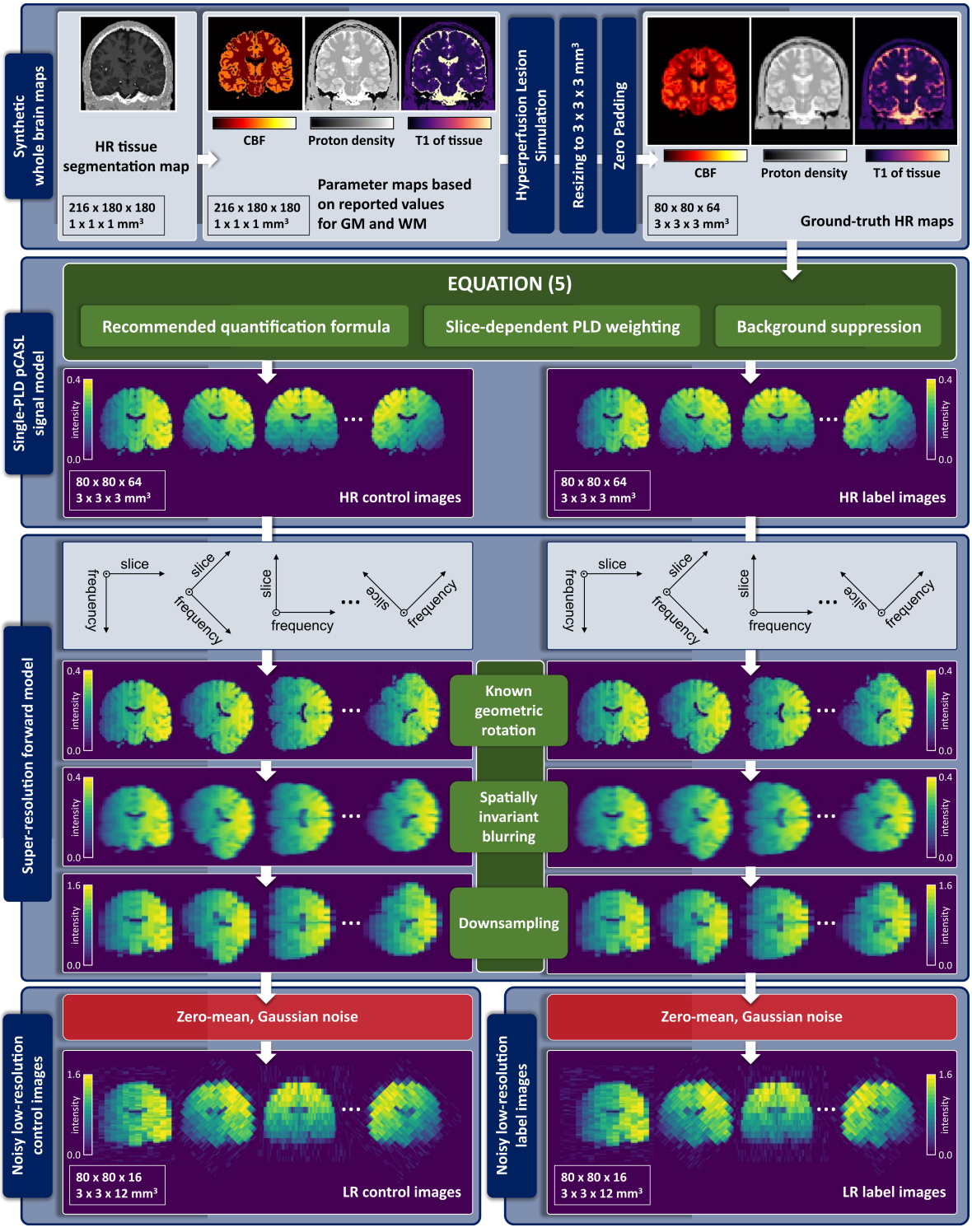

Figure S2: A flowchart of the data simulation process for single-PLD pCASL data using SRR, in correspondence with the procedure outlined in Section 3.1. Coronal slices are shown for four slice-encoding directions, illustrating the forward modelling of HR ground-truth parameter maps to LR MS images. Signal intensities of the control and label images are shown in arbitrary units.

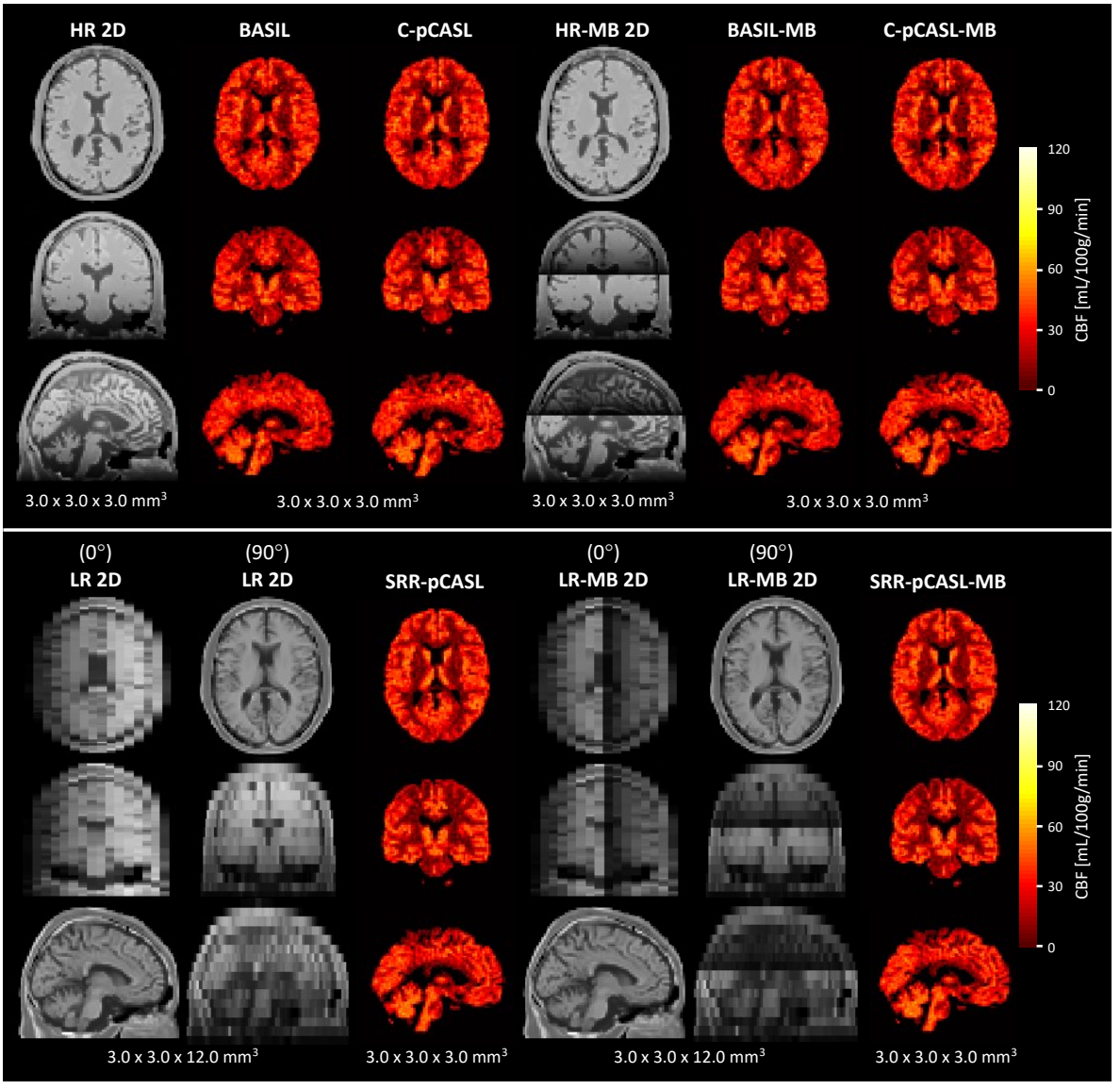

Figure S3: Orthogonal slice views of simulated HR 2D control images with high through-plane resolution ($3 \times 3 \times 3$ mm^3), without multiband (top panel, column 1) and with multiband (top panel, column 4), and simulated LR 2D control images with low through-plane resolution ($3 \times 3 \times 12$ mm^3), without multiband (bottom panel, columns 1-2) and with multiband (bottom panel, columns 4-5). For illustration purposes, only two slice orientation angles (0° and 90°) are shown for the 2D LR control images (see also Fig. 1). Simulated control images are compared to the corresponding HR CBF map estimates reconstructed with BASIL (top panel, column 2), C-pCASL (top panel, column 3), BASIL-MB (top panel, column 5), C-pCASL-MB (top panel, column 6), and the proposed SRR-pCASL (bottom panel, column 3) and SRR-pCASL-MB (bottom panel, column 6), respectively.

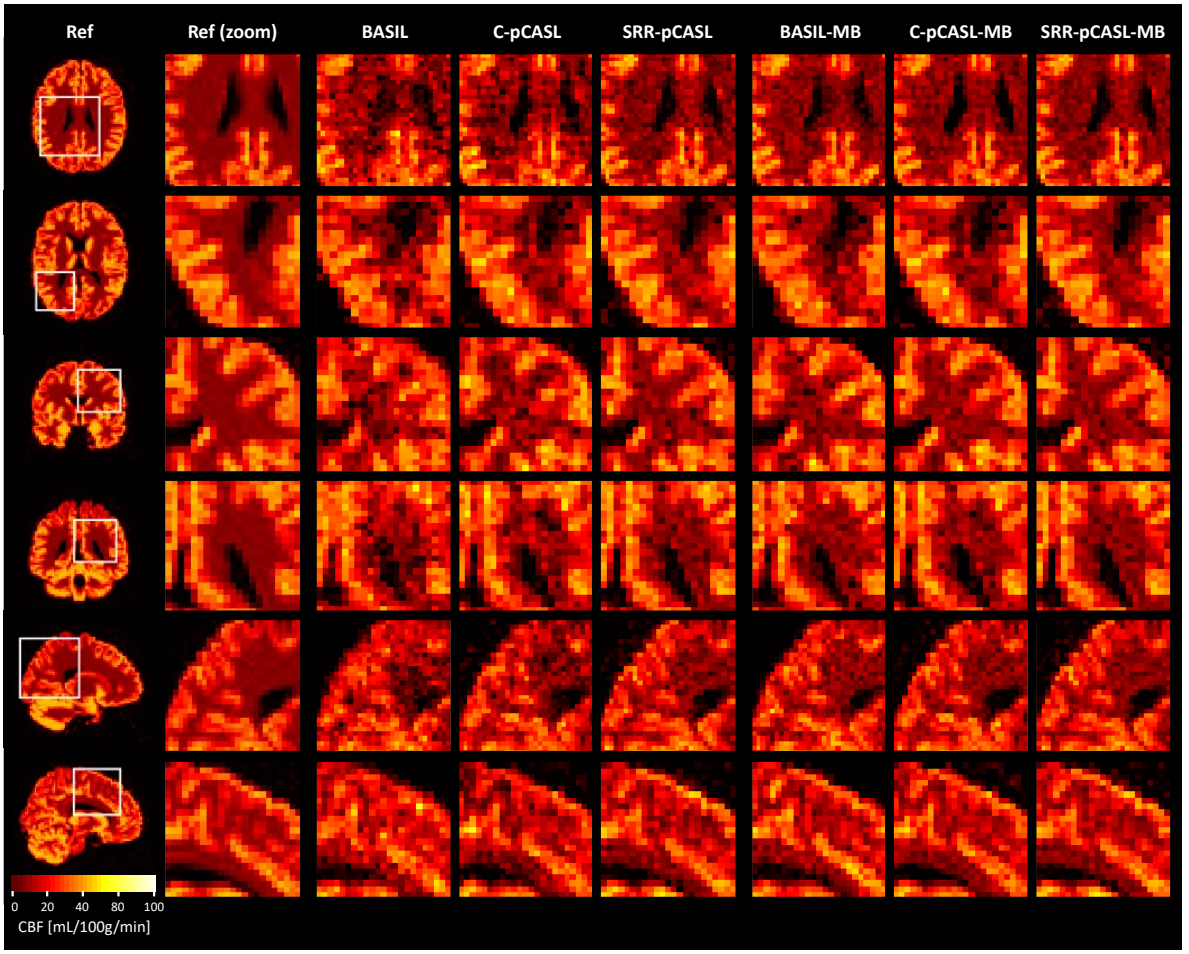

Figure S4: Orthogonal slice views with zoomed close-ups showing the high-resolution CBF map estimated with BASIL (column 3), C-pCASL (column 4), BASIL-MB (column 6), C-pCASL-MB (column 7), and the proposed SRR-pCASL (column 5) and SRR-pCASL-MB (column 8), compared to the ground truth CBF map as a reference (columns 1-2) for the whole brain simulation experiment **without motion**.

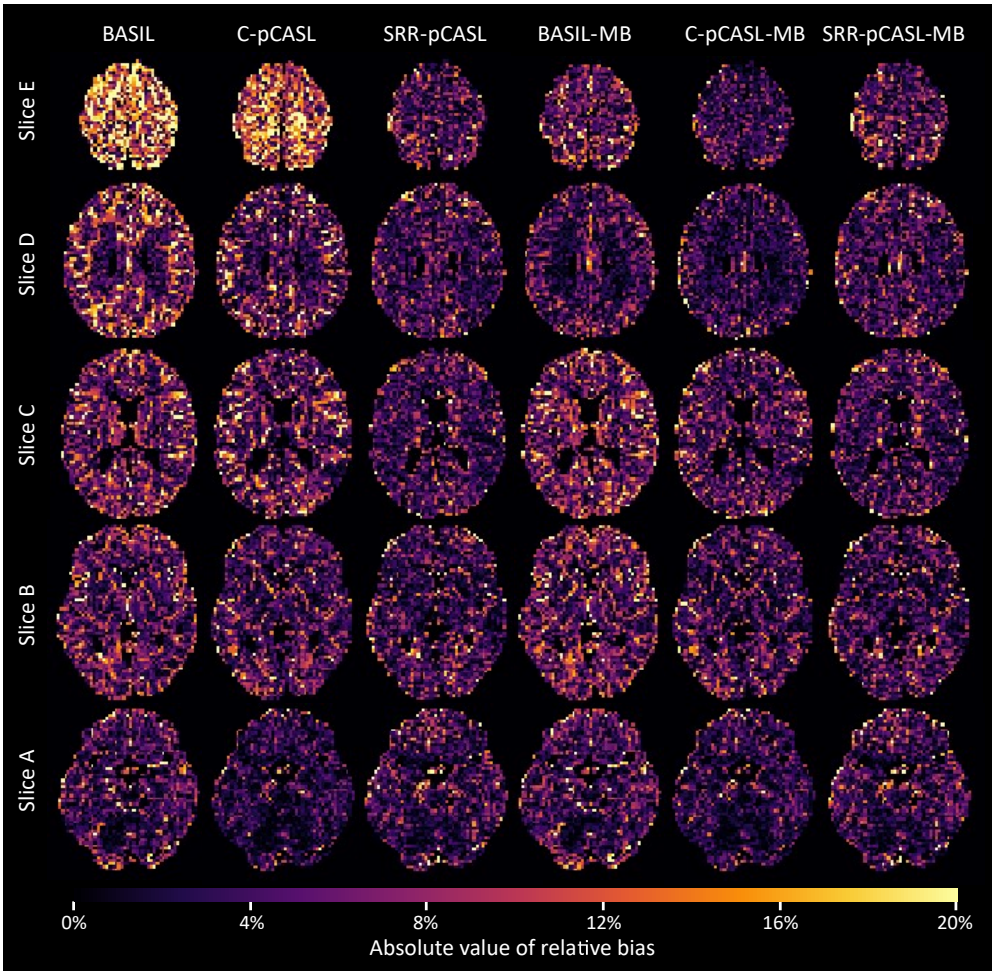

Figure S5: Absolute value of relative bias maps for CBF, calculated from the reconstruction results of the synthetic whole brain simulations **without motion**. For each method, five transverse slices are shown, corresponding with the slice letter convention in Fig. 5 of the main body.

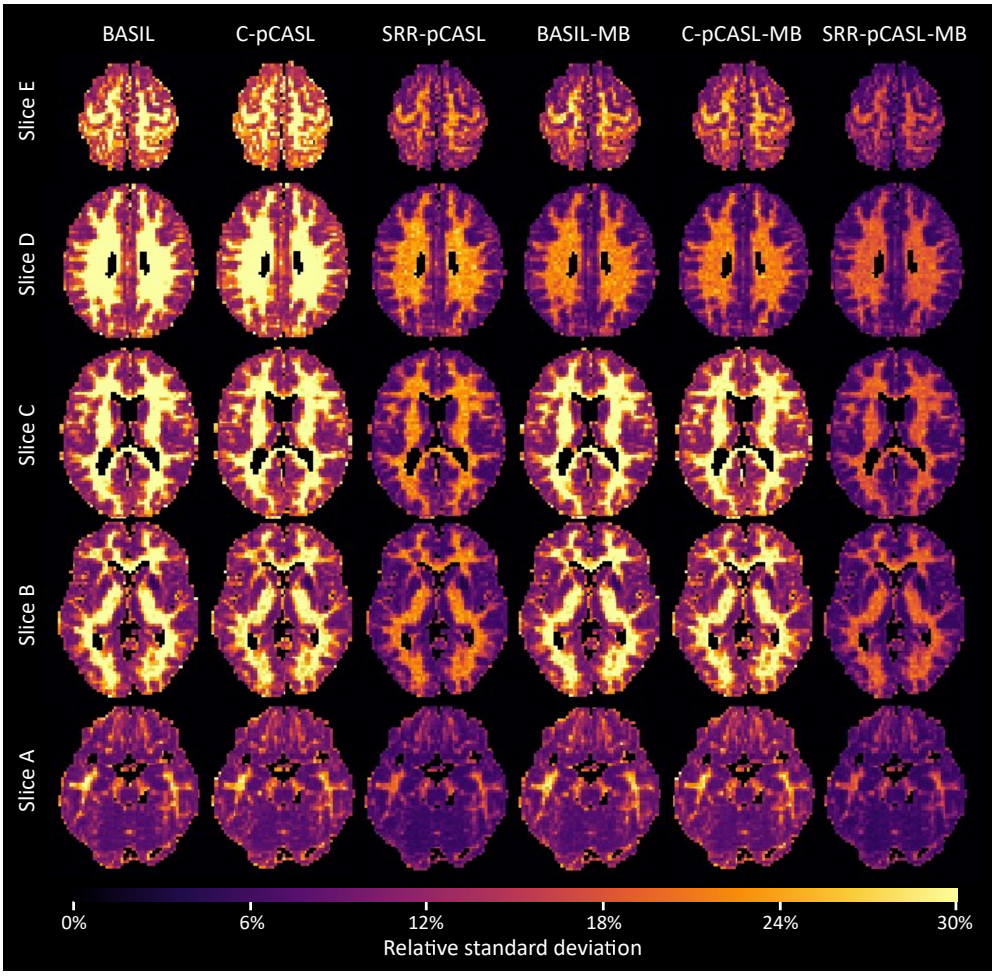

Figure S6: Relative standard deviation maps for CBF, calculated from the reconstruction results of the synthetic whole brain simulations **without motion**. For each method, five transverse slices are shown, corresponding with the slice letter convention in Fig. 5 of the main body.

Table S1
Acquisition settings for the synthetic data set using 2D MS readout, that was used for the additional simulation experiment with adjusted resolution. A slice orientation angle of 0° corresponds with the slice-encoding axis directed from left to right, and with the phase-encoding axis perpendicularly directed from anterior to posterior. Each angle listed below is a rotation of the slice-encoding axis around the phase-encoding direction counterclockwise. Therefore, a 90° angle is consistent with an ascending slice order. These rotations are consistent with the rotations visualized in Fig. 1 of the main body.

	Extra Dataset LR 2D MS
Number of slices per slab N_{slice}	12
Acquisition matrix	120 × 120
FOV [mm^3]	240 × 240 × 192
Voxel size [mm^3]	2 × 2 × 16
Labeling duration τ [ms]	1800
PLD_{base} [ms]	1800
PLD range [ms]	1800-2350
Number of control-label pairs N	24
Number of slice encoding directions	24
Slice orientation angles [°]	0, 7.5, . . . , 172.5
Multiband factor ω	n.a.

Next, to demonstrate that the potential of super-resolution reconstruction (SRR) is not confined to a particular resolution, an additional simulation experiment was performed where a $2\times2\times2$ mm^3 CBF map was super-resolution reconstructed from LR images with a resolution of $2\times2\times16$ mm^3. Acquisition settings for this addition simulation experiment are summarized in Table S1. Fig. S7 shows the result of this extra simulation experiment side-by-side with the original simulation experiment where a $3\times3\times3$ mm^3 CBF was reconstructed.

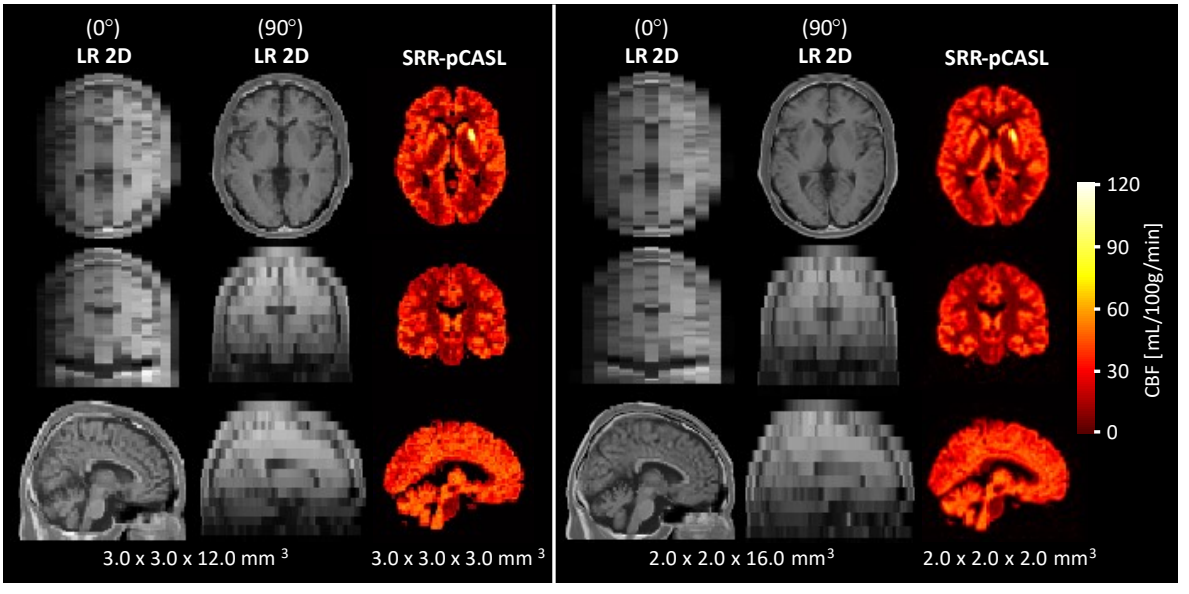

Figure S7: Orthogonal slice views of simulated LR 2D control images with low through-plane resolution compared to the HR CBF map estimates reconstructed with SRR-pCASL, for the original acquisition protocol using LR images with a resolution of $3\times3\times12$ mm^3 as input (left), and the new acquisition protocol using LR images with a resolution of $2\times2\times16$ mm^3 as input (right), as summarized in Table S1. For illustration purposes, only the slice orientation angles corresponding with a slice orientation of 0° and 90° are shown for the 2D LR control images (see also Fig. 1).

S1.2. Simulations with motion

To ease a qualitative and visual comparison of the CBF map estimates for each method in the whole brain simulation experiment with motion, Fig. S8 shows zoomed image regions to indicate noticeable CBF estimation differences compared to the ground truth CBF map (Ref). Furthermore, Fig. S9 and Fig. S10 show axial slices of the relative absolute bias and relative standard deviation maps for the simulation experiment with motion, corresponding with the slice locations of Fig. 5 of the main body.

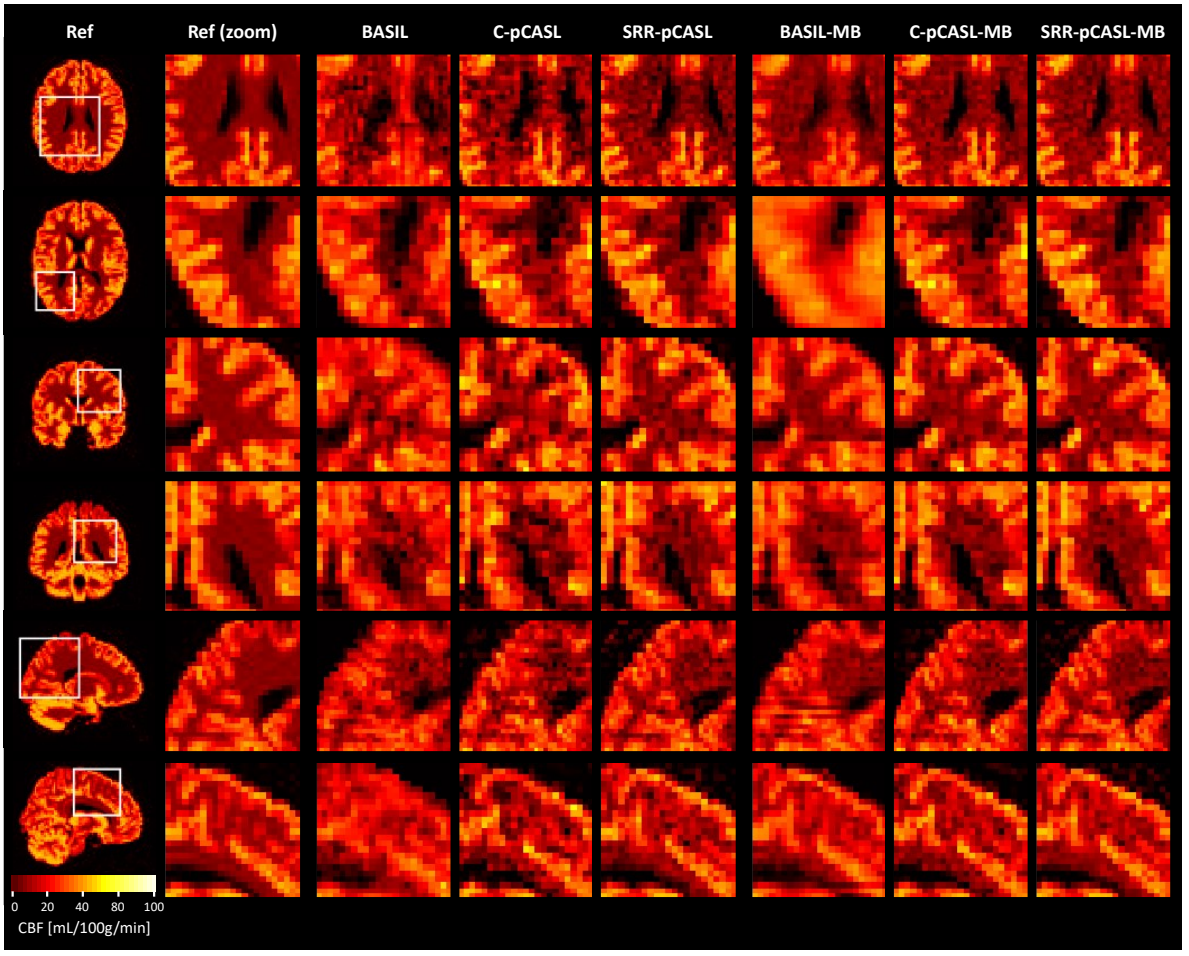

Figure S8: Orthogonal slice views with zoomed close-ups showing the high-resolution CBF map estimated with BASIL (column 3), C-pCASL (column 4), BASIL-MB (column 6), C-pCASL-MB (column 7), and the proposed SRR-pCASL (column 5) and SRR-pCASL-MB (column 8), compared to the ground truth CBF map as a reference (columns 1-2) for the whole brain simulation experiment **with motion**.

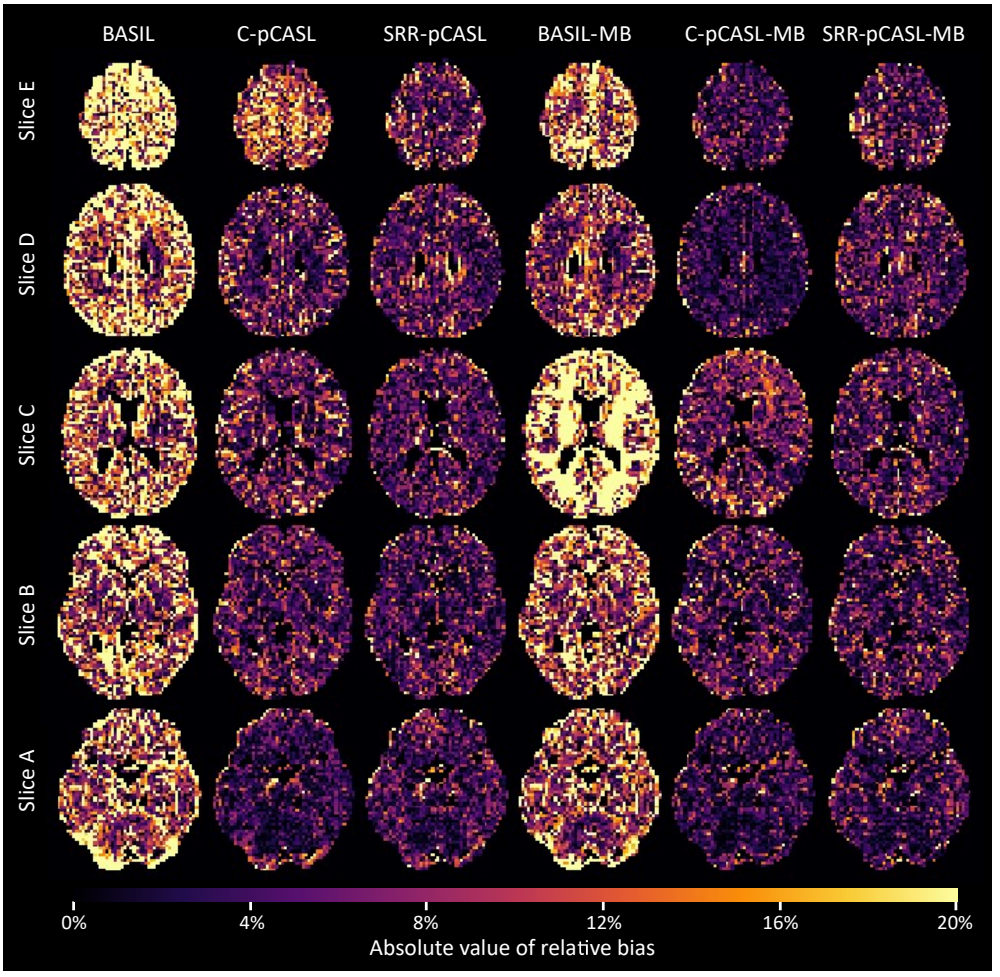

Figure S9: Absolute value of relative bias maps for CBF, calculated from the reconstruction results of the synthetic whole brain simulations **with motion**. For each method, five transverse slices are shown, corresponding with the slice letter convention in Fig. 5 of the main body.

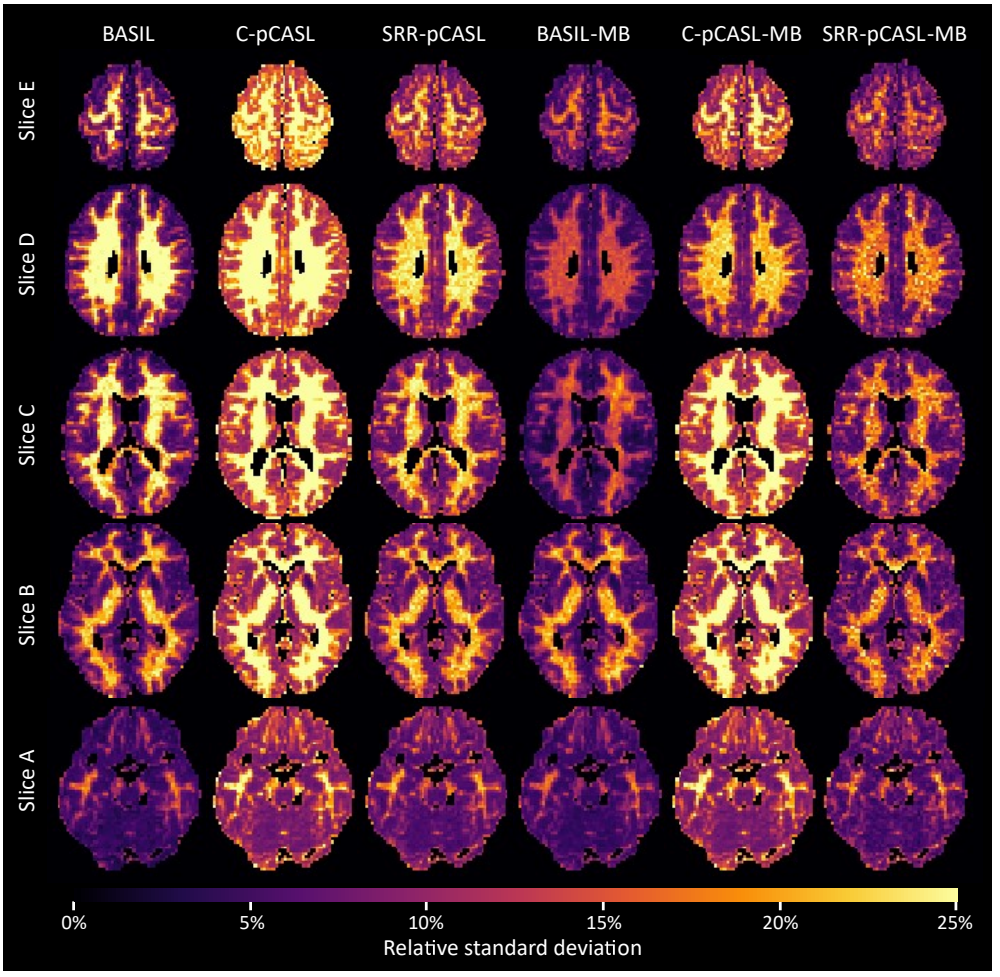

Figure S10: Relative standard deviation maps for CBF, calculated from the reconstruction results of the synthetic whole brain simulations **with motion**. For each method, five transverse slices are shown, corresponding with the slice letter convention in Fig. 5 of the main body.

Fig. S11 and Fig. S12 summarize the motion parameter estimates for the simulation experiment with motion, both without and with the use of multiband. Each figure shows the true reference motion component values $\boldsymbol{\theta}_n = \{\theta_{nk}\}_{k=1}^{6}$ being used to corrupt each image number, $n = 1 \dots 2N$, in the whole brain simulations with added motion. To guarantee realistic head movement, the reference motion set $\boldsymbol{\theta}_n$ was obtained from the *in vivo* LR SRR data using a procedure that involved three repetitions of: (i) upsampling of the LR SRR data by applying the adjoint operator $\boldsymbol{A}_n^T = \boldsymbol{M}_{\boldsymbol{\theta}_n}^T \boldsymbol{G}_n^T \boldsymbol{B}^T \boldsymbol{D}^T$ to each LR control and label image, (ii) calculation of the average HR control and rCBF maps from this upsampled data using the recommended quantification formula in Eq. (2) of the main body paper and averaging over the number of control-label pairs N, and (iii) motion estimation using subproblem (P.2) in the main body in which the HR control and rCBF map remained fixed. The motion parameters that resulted from this procedure were then used as reference motion component values. Next, Fig. S11 and Fig. S12 also show the mean motion parameter component $\overline{\theta}_{nk}$, where the mean was calculated over the N_{MC} estimates for each image number n. In addition, for each component and framework combination, the RMSE was plotted using a barplot, where the RMSE value was calculated per motion component as:

$$\mathrm{RMSE}(\theta_{nk}) = \left(\overline{\left(\theta_{nk} - \overline{\theta}_{nk} \right)^2} \right)^{\frac{1}{2}}, \tag{S1}$$

where $\overline{\theta}_{nk}$ denotes the sample mean of the N_{MC} estimates of the motion component k for image number n, and where $\overline{(\cdot)}$ denotes the element-wise sample mean operator over the N_{MC} estimates. Note that, in line with the definitions in Section 2.2 of the main body paper, pCASL images $\boldsymbol{r}_n$ were pairwise ranked in alternating order as control-label-control-label-… . As highlighted by the red bars in Fig. S11 and Fig. S12, the control-label image pair corresponding with image numbers 39 and 40 was discarded from the CBF quantification routine in BASIL and BASIL-MB due to consistent outliers of the estimated motion parameter components that resulted from the pre-registration routine using FSL's *mcflirt*.

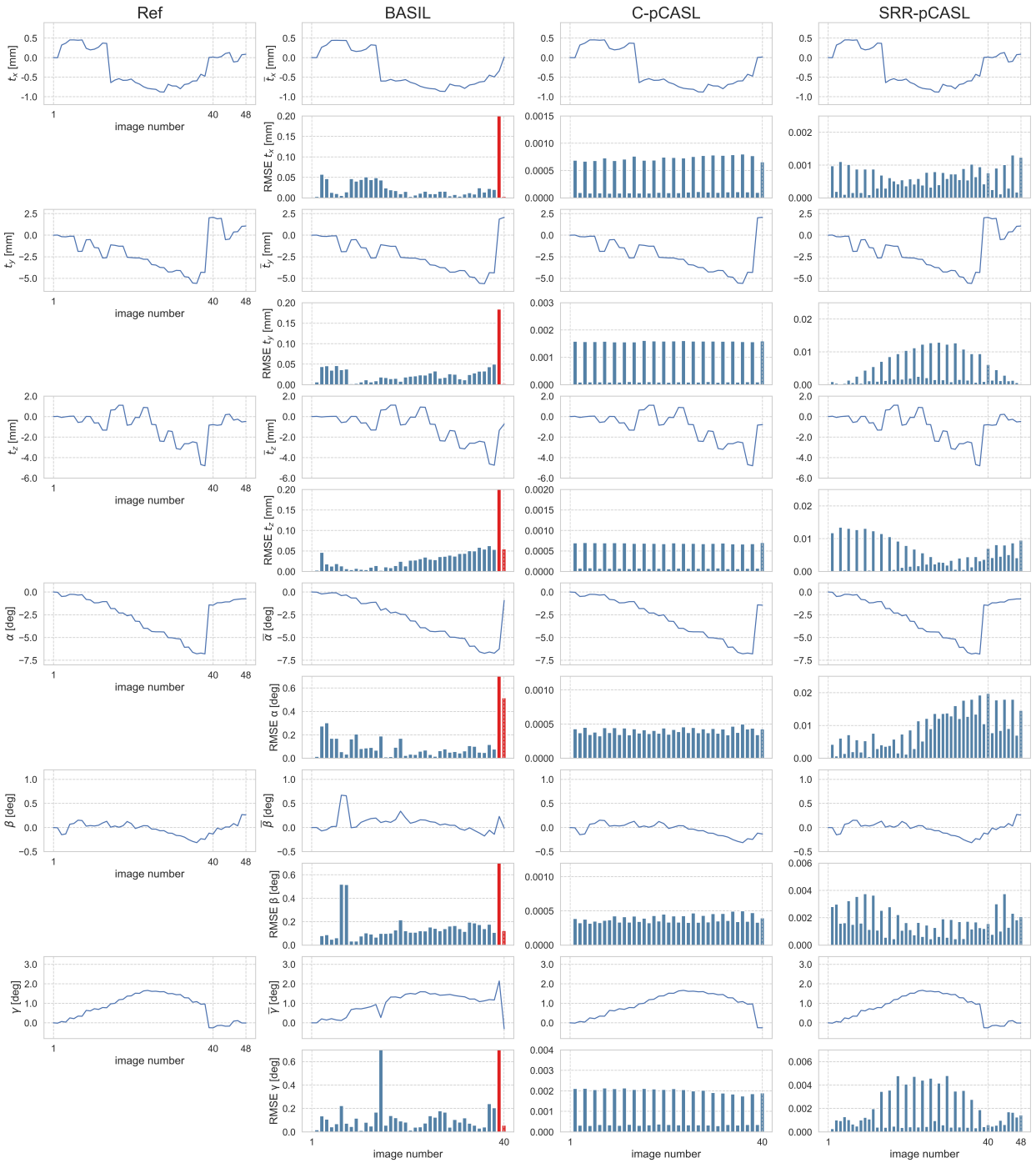

Figure S11: Graphs of the mean motion component estimate and associated RMSE, for each image number and respective framework **without the use of multiband**, calculated over the $N_{\text{MC}} = 100$ results for the whole brain simulation experiment with motion. The true reference values for each motion component are shown in column 1. The outlier discarded control-label image pair for BASIL is annotated in red.

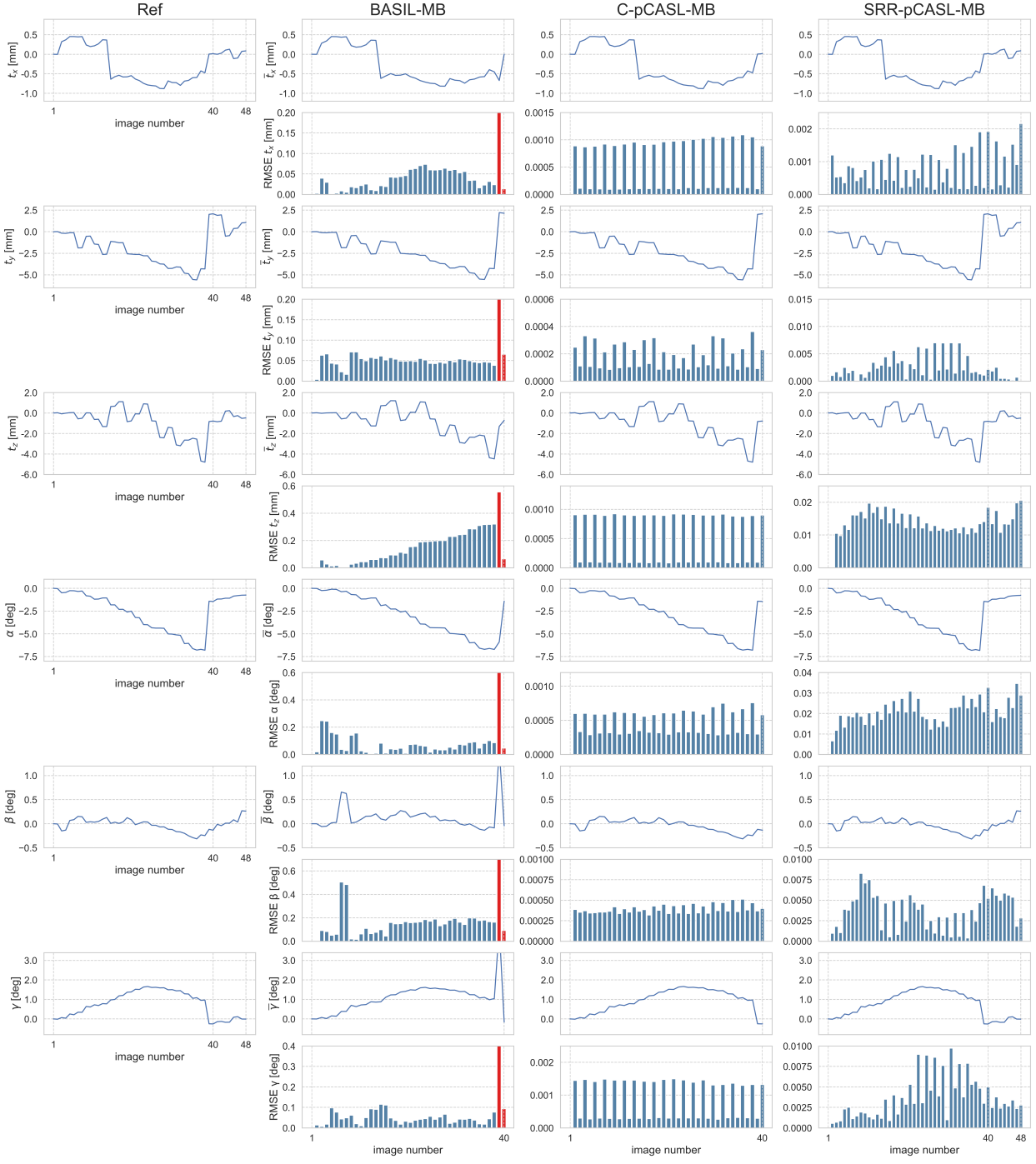

Figure S12: Graphs of the mean motion component estimate and associated RMSE, for each image number and respective framework **using multiband**, calculated over the $N_{\text{MC}} = 100$ results for the whole brain simulation experiment with motion. The true reference values for each motion component are shown in column 1. The outlier discarded control-label image pair for BASIL-MB is annotated in red.